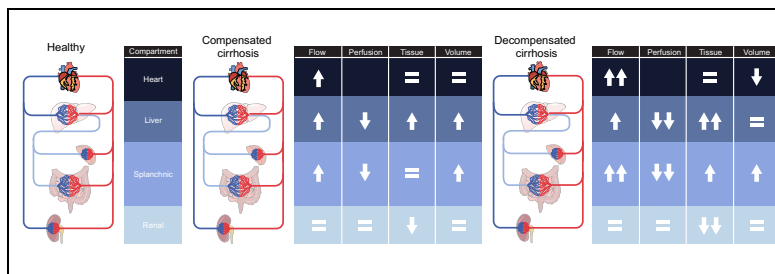


# Multi-organ assessment of compensated cirrhosis patients using quantitative magnetic resonance imaging

## Graphical abstract



## Authors

Christopher R. Bradley, Eleanor F. Cox, Robert A. Scott, ..., Guruprasad P. Aithal, Susan T. Francis, Indra Neil Guha

## Correspondence

Neil.Guha@nottingham.ac.uk  
(I.N. Guha)

## Highlights

- Assessment of MRI parameters in a single scan session.
- Higher liver  $T_1$  and reduced liver perfusion with increasing disease severity and clinical outcomes.
- Reduced renal cortex  $T_1$  linked to disease severity and clinical outcomes.

## Lay summary

This study assesses the changes to structure, blood flow and perfusion that occur in the key organs (liver, spleen and kidney) associated with severe liver disease (Compensated Cirrhosis), using magnetic resonance imaging. The magnetic resonance imaging measures which changed with disease severity and were related to negative liver-related clinical outcomes are described.



## Multi-organ assessment of compensated cirrhosis patients using quantitative magnetic resonance imaging

Christopher R. Bradley<sup>1,2</sup>, Eleanor F. Cox<sup>1,2</sup>, Robert A. Scott<sup>2</sup>, Martin W. James<sup>2</sup>, Phillip Kaye<sup>2</sup>, Guruprasad P. Aithal<sup>2,3</sup>, Susan T. Francis<sup>1,2,†</sup>, Indra Neil Guha<sup>2,3,\*,†</sup>

<sup>1</sup>Sir Peter Mansfield Imaging Centre, School of Physics and Astronomy, University of Nottingham, Nottingham, UK; <sup>2</sup>NIHR Biomedical Research Centre, Nottingham University Hospitals NHS Trust and the University of Nottingham, Nottingham, UK; <sup>3</sup>Nottingham Digestive Diseases Centre, School of Medicine, University of Nottingham, Nottingham, UK

See Editorial, pages 996–998

**Background & Aims:** Advancing liver disease results in deleterious changes in a number of critical organs. The ability to measure structure, blood flow and tissue perfusion within multiple organs in a single scan has implications for determining the balance of benefit vs. harm for therapies. Our aim was to establish the feasibility of magnetic resonance imaging (MRI) to assess changes in Compensated Cirrhosis (CC), and relate this to disease severity and future liver-related outcomes (LROs).

**Methods:** A total of 60 patients with CC, 40 healthy volunteers and 7 patients with decompensated cirrhosis were recruited. In a single scan session, MRI measures comprised phase-contrast MRI vessel blood flow, arterial spin labelling tissue perfusion, T<sub>1</sub> longitudinal relaxation time, heart rate, cardiac index, and volume assessment of the liver, spleen and kidneys. We explored the association between MRI parameters and disease severity, analysing differences in baseline MRI parameters in the 11 (18%) patients with CC who experienced future LROs.

**Results:** In the liver, compositional changes were reflected by increased T<sub>1</sub> in progressive disease ( $p < 0.001$ ) and an increase in liver volume in CC ( $p = 0.006$ ), with associated progressive reduction in liver ( $p < 0.001$ ) and splenic ( $p < 0.001$ ) perfusion. A significant reduction in renal cortex T<sub>1</sub> and increase in cardiac index and superior mesenteric arterial blood flow was seen with increasing disease severity. Baseline liver T<sub>1</sub> ( $p = 0.01$ ), liver perfusion ( $p < 0.01$ ), and renal cortex T<sub>1</sub> ( $p < 0.01$ ) were significantly different in patients with CC who subsequently developed negative LROs.

**Conclusions:** MRI enables the contemporaneous assessment of organs in liver cirrhosis in a single scan without the requirement for a contrast agent. MRI parameters of liver T<sub>1</sub>, renal T<sub>1</sub>, hepatic and splenic perfusion, and superior mesenteric arterial blood flow were related to the risk of LROs.

**Lay summary:** This study assesses the changes to structure, blood flow and perfusion that occur in the key organs (liver, spleen and kidney) associated with severe liver disease (Compensated Cirrhosis), using magnetic resonance imaging. The magnetic resonance imaging measures which changed with disease severity and were related to negative liver-related clinical outcomes are described.

© 2018 European Association for the Study of the Liver. Published by Elsevier B.V. This is an open access article under the CC BY-NC-ND license (<http://creativecommons.org/licenses/by-nc-nd/4.0/>).

### Introduction

The evolution of liver cirrhosis to clinical liver-related outcomes resulting from portal hypertension is not simply dictated by architectural and haemodynamic changes within the liver. Rather, advancing liver disease results in deleterious changes in a number of critical organs and the understanding of this process is a central aspect in the clinical management of cirrhotic patients.

The hyperdynamic circulation in cirrhosis is characterised by increased cardiac output and decreased systemic vascular resistance with low arterial blood pressure.<sup>1–3</sup> Splanchnic vasodilation, with a resulting decrease in the effective central volume, has been proposed as an important driver of the hyperdynamic circulation.<sup>1,4</sup> Associated with splanchnic vasodilation is an increase in portal vein blood flow which maintains and perpetuates portal hypertension.<sup>5</sup> Further, architectural and haemodynamic changes in the heart, spleen, and kidney have also been shown to occur and have important pathophysiological consequences. For example, cirrhotic cardiomyopathy is characterised by increased cardiac output with a sub-optimal ventricular response to stress, and structural and electrophysiological abnormalities.<sup>2</sup> Cardiac dysfunction associated with cirrhosis has been shown to be an important prognostic determinant of mortality at one year.<sup>6</sup> Renal vasoconstriction, related to splanchnic vasodilation, portal hypertension and activation of compensatory neurohormonal systems, is a precursor for the development of hepatorenal syndrome.<sup>3,6,7</sup> In cirrhosis, splenic enlargement may result from portal venous congestions and/or hyperplasia. In association, the splenic artery is suggested to dilate,<sup>8</sup> and recent data suggests that the splenic artery to hepatic artery diameter ratio can predict the development of

Keywords: Compensated Cirrhosis; Magnetic Resonance Imaging; Arterial Spin Labelling; Phase contrast; Longitudinal T<sub>1</sub> relaxation time.

Received 2 January 2018; received in revised form 29 May 2018; accepted 30 May 2018; available online 08 June 2018

\* Corresponding author. Address: National Institute for Health Research (NIHR) Nottingham Biomedical Research Centre, Nottingham University Hospitals NHS Trust and University of Nottingham, E Floor, West Block QMC, Queens Medical Centre, Nottingham NG7 2UH, UK. Tel.: +44 (0) 115 8231162.

E-mail address: [Neil.Guha@nottingham.ac.uk](mailto:Neil.Guha@nottingham.ac.uk) (I.N. Guha).

† Joint senior authors.



ascites and varices.<sup>9</sup> Splenic stiffness has also been found to have a strong association with portal hypertension.<sup>10,11</sup> However, there is an incomplete understanding of how changes in the different organs are inter-related, and what temporal relationships exist.

The importance of assessing critical organs in liver cirrhosis in a holistic fashion is illustrated by the current controversy surrounding beta-blockers in liver cirrhosis. The debate regarding the safety of beta-blockers focusses on whether the beneficial effects of beta-blockers in liver cirrhosis, centred around a reduction in cardiac output, splanchnic vasodilation and portal inflow and improvement in intrahepatic resistance (alpha 1 blockade), is counterbalanced by deleterious effects in advanced cirrhosis centred on a reduction in renal perfusion and cardiac output as described previously.<sup>12</sup> A key limitation in being able to define the critical window<sup>5,13</sup> of benefit of beta-blockers vs. harm is the lack of robust non-invasive tools to measure changes across organs in a contemporaneous manner. If this could be done, treatment could be individualised more effectively. This does not currently occur in clinical practice, in a consistent manner, as the tools for measurement are blunt (e.g. heart rate) or invasive (hepatic venous pressure gradient measurement [HVPG]).

Recent advances in non-invasive magnetic resonance imaging (MRI) techniques allow the assessment of blood flow to organs,<sup>14</sup> tissue perfusion,<sup>15,16</sup> and compositional changes including fibrosis and inflammation,<sup>17–19</sup> in the key organs associated with cirrhosis. Until now, such measures have only been examined in single organs rather than using a comprehensive multi-organ approach in a single scan session.

Our aim was to assess the feasibility of performing MRI to contemporaneously analyse the liver, heart, spleen and kidneys in patients with Compensated Cirrhosis (CC). We aim to describe the differences in quantitative MRI measures within these organs between healthy volunteers, and patients with CC and Decompensated Cirrhosis (DC). As proof of concept, we explore whether differences in MRI parameters are observed in patients with future clinical liver-related outcomes.

## Materials and methods

### Study population

Sixty patients were consecutively recruited from a CC cohort study, a prospective study initiated in 2010 focussed on tracking liver disease progression. Here, baseline measures collected for this cohort are reported. Institutional and local research approval was gained (10/H0403/10). Patients were recruited with evidence of cirrhosis (confirmed by a combination of biopsy, clinical and radiological criteria) and no evidence of decompensation (ascites, significant jaundice, hepatic encephalopathy and variceal bleeding), hepatocellular carcinoma and portal vein thrombosis. Exclusion criteria included orthotopic liver transplantation, ischaemic heart disease, alcoholic cardiomyopathy (defined by clinical evidence of systolic dysfunction) and valvular heart disease.

For comparator measures, we prospectively recruited two additional groups – a Healthy Volunteer (HV) and Decompensated Cirrhosis (DC) group. Forty HVs were recruited who had no major co-morbidity including cardiovascular or chronic liver disease. Seven ambulatory patients with DC were recruited, defined as Baveno 3 or 4 stage (ascites, encephalopathy or previous variceal bleed); exclusion criteria included portal vein

thrombosis, the presence of hepatocellular carcinoma (HCC), and orthotopic liver transplantation. Subjects attended on a single study day following an overnight fast. Statistical power to assess the difference between groups was determined for each MRI parameter at a power of 80% and significance level of 5%.

Patients were invited to return for research visits on a six-monthly basis for assessment of liver-related clinical outcomes as defined by ascites (needing paracentesis or diuretic therapy), grade 3 or grade 4 encephalopathy, variceal haemorrhage requiring endoscopic therapy and emergency admission, HCC (defined by EASL criteria) and liver-related death. For patients who declined follow-up visits, we obtained their consent to access relevant medical records (both family practitioner and hospital records) to record clinical outcomes.

### Multi-organ MRI protocol

All participants were scanned following a 6 h fast, with MRI scans carried out between 8 am–12 pm. Imaging was performed on a 1.5 T Philips Achieva MRI scanner (Best, Netherlands) using a 16-element Torso receive coil and body transmit coil. MR measures were collected on four organs: liver – blood flow in the portal vein and hepatic artery, liver perfusion and tissue T<sub>1</sub>; spleen and superior mesenteric artery (SMA) – blood flow assessed in the splenic and SMA, splenic tissue perfusion and tissue T<sub>1</sub>; renal – blood flow in right renal artery, kidney volume, renal tissue perfusion and tissue T<sub>1</sub>; heart – aortic blood flow corrected for body surface area (BSA) to yield cardiac index and left ventricular (LV) wall mass as a measure of cardiac strain. This non-invasive protocol took less than 1 h for hepatic (~20 min), spleen, SMA and renal (~15 min), and cardiac (~10 min) measures. The following describes the acquisition protocol parameters.

#### Organ volume

First multi-slice balanced turbo-field echo (bTFE) localiser images were acquired in three perpendicular orientations to locate organs and vessels of interest for slice positioning, and from which to estimate organ (liver, kidney and spleen) volume.

#### Blood flow measures

Phase-contrast (PC)-MRI was used to quantify vessel lumen cross-sectional area (CSA), velocity and bulk blood flow in vessels within each system. A TFE technique (two averages, TFE factor 4–6 dependent on subjects' heart rate) was used with a single slice perpendicular to the vessel of interest. A total of 15 phases were collected across the cardiac cycle using specified velocity encoding for each vessel (portal vein 50 cm/s, hepatic/splenic/renal arteries 100 cm/s, SMA 140 cm/s). Each vessel measurement was acquired during a 15–20 s breath hold.

#### Perfusion of the liver, spleen and kidney

Respiratory-triggered Flow Alternating Inversion-Recovery Arterial Spin Labelling (FAIR-ASL)<sup>15,16</sup> (post-labelling delay 1,100 ms, balanced fast field echo [bFFE] readout) was used to measure tissue perfusion in the liver, spleen and renal tissue. Liver perfusion data was acquired in three sagittal slices through the right lobe (slice gap 5 mm, 60 ASL pairs in ~8 min), spleen/renal perfusion data was collected in five contiguous coronal-oblique slices through the spleen and long axis of the kidney (30 ASL pairs in ~5 mins). An equilibrium base magnetisation M<sub>0</sub> and T<sub>1</sub> image was acquired for each slice orientation for perfusion quantification.

*Relaxometry of the liver, spleen and kidney*

A modified respiratory-triggered inversion-recovery sequence<sup>16,19,20</sup> was used to measure tissue  $T_1$  in the liver, spleen and kidney, with slices geometrically matched to the ASL data. For liver tissue, a fat suppressed spin-echo echo-planar imaging (SE-EPI) readout was used to ensure no influence of fat on  $T_1$  measures. Data was collected at 13 inversion times (TI) (100–1,200 ms in 100 ms steps, and 1,500 ms) with minimal temporal slice spacing between the three slices (65 ms) collected in a descend slice order, in an acquisition time of ~2 min. For the spleen and kidney, a bFFE readout was used and data acquired at 9 TIs (100–900 ms in 100 ms steps) with minimal temporal slice spacing (144 ms), both ascend and descend slice order acquisitions were acquired to increase the dynamic range of inversion times<sup>16,19,20</sup> in ~3 min. It was confirmed that study participants did not have excess iron.<sup>16,19,20</sup>

*Cardiac assessment*

Cardiac output was measured using a PC-MRI of the aorta with 30 phases and velocity encoding of 200 cm/s in ~1 min whilst free breathing. Short-axis cine images were acquired to measure LV wall mass using a multi-slice TFE sequence (12 slices, 30 phases, 3 slices acquired per 15–20 s breath hold).

**Data analysis**

*Blood flow measures*

'Q-flow' software (Philips Medical Systems) was used to analyse PC-MRI data. For each vessel, a region-of-interest (ROI) was drawn to estimate flow by averaging the flow velocity values within the ROI and multiplying by vessel lumen CSA. Mean flow was calculated by averaging the flow rates for each cardiac phase across the cardiac cycle.

*Perfusion*

The analysis procedure for ASL data performed using MATLAB and/or IDL routines is shown (Fig. S1). Each ASL label/control image was motion corrected to the base magnetisation  $M_0$  image using in-house software. Individual perfusion-weighted images (control-label) were calculated, inspected for motion (exclude >1 voxel movement) and averaged to create a single perfusion-weighted image ( $\Delta M$ ).  $\Delta M$ ,  $M_0$  and  $T_1$  maps were used in a kinetic model<sup>21</sup> to compute tissue perfusion maps. A binary mask of each organ (see *relaxometry* section) was formed and used to calculate the mean liver, spleen and renal cortex perfusion.

*Relaxometry*

Inversion-recovery data were fit to a two-parameter model to generate  $T_1$  and  $M_0$  maps. Binary organ masks were formed from the  $M_0$  image, and major blood vessels further segmented by excluding voxels with a  $T_1 > 1,500$  ms. Median  $T_1$  values were calculated within liver and spleen masks. For the kidney mask, a histogram of  $T_1$  values was formed to yield two peaks originating from the renal cortex and medulla (Fig. S1A), and the median  $T_1$  values of the renal cortex and medulla calculated.

*Volume*

Analyze<sup>®</sup> (Mayo Clinic) was used to draw an ROI around each organ (liver, kidney, spleen) within each slice, and total organ volume calculated by summing across slices.

*Cardiac*

Cardiac MRI data was analysed using ViewForum software (Philips Medical Systems, Best, Netherlands). PC-MRI data of the aorta was analysed by computing the stroke volume and heart rate, and multiplying these parameters to yield cardiac output. This software was also used to draw wall contours from which LV wall mass was calculated. Both cardiac output and LV wall mass are presented corrected for BSA.<sup>22</sup>

**Validation of MR measures**

*$T_1$  relaxometry of the liver*

We assessed liver histology in a cohort of patients with cirrhosis who previously had  $T_1$  mapping of the liver on a 1.5 T scan,<sup>19,20</sup> all MRI scans were collected within three months of liver biopsy. Liver biopsies were obtained via either the percutaneous or the transjugular route from patients with METAVIR fibrosis stage 4. Patients were fasted overnight before the procedure and biopsies were carried out by experienced operators. Biopsies were stained with hematoxylin and eosin, picosirius red (PSR) and Perls' Prussian blue stains. All biopsy data were analysed by a single experienced pathologist blinded to MRI data. The percentage of fibrous tissue relative to the total biopsy area was estimated for each biopsy by visual morphometry.<sup>17</sup> A Spearman's rank correlation coefficient (in terms of R value) was computed between the continuous variables of visual morphometry and liver tissue  $T_1$ .

All patients with CC had a blood sample to assess non-invasive markers of liver fibrosis (Enhanced Liver Fibrosis [ELF] score). In addition, in all patients with CC, transient elastography evaluation was performed using FibroScan<sup>®</sup> (EchoSens, Paris, France) to provide a liver stiffness measure (LSM) in kPa. The FibroScan<sup>®</sup> measure was repeated to obtain 10 readings and a median LSM value calculated. Spearman's rank correlation coefficients (R value) are presented between ELF and LSM with a statistical significance threshold of  $p < 0.05$ .

*ASL perfusion of the liver*

In all patients, measures of indocyanine green (ICG) were performed and plasma disappearance rate (ICG-PDR, percentage of ICG eliminated in 1 min after an ICG bolus) (%/min), and its retention rate at 15 min (ICGR15, the circulatory retention of ICG during the first 15 min after a bolus injection (%)) computed. A Spearman's rank correlation coefficient was performed between ICG-PDR and ICGR15 and liver perfusion as measured using arterial spin labelling. Correlation coefficients are presented in terms of R value with a statistical significance threshold of  $p < 0.05$ .

*Repeatability of multiparametric MRI measures*

To determine the between session repeatability of MRI measures, the intra-subject Coefficient of Variation (CoV) (defined as the standard deviation/mean) of multiparametric MRI measures were assessed. A subset of 10 healthy participants (age 23–37 years, body mass index 20–26 kg/m<sup>2</sup>) had three scans, at least one week apart and within four weeks, at the same time of day and after an overnight fast to limit diurnal and dietary variability. The CoV measures are provided (Table S1).

**Statistical analysis**

All statistical analysis was performed using Prism 6 (GraphPad Software, Inc., La Jolla, CA). A Shapiro-Wilk normality test was applied to data collected on each MRI parameter. Normal data

is expressed as mean (SEM) and non-normal as median (interquartile range, IQR) across each group. Tests between the three patient groups were made using a one-way analysis of variance (one-way ANOVA) with Bonferroni correction for normally distributed data, otherwise a Kruskal-Wallis test was performed to assess probable differences between the groups, with *post hoc* Tukey's test where significant differences were identified.

To compare results between patients with CC who did or did not have a negative liver-related clinical outcome, a two-tailed unpaired *t* test was performed to assess differences in normally distributed parameters, or a Mann-Whitney U test was performed, significance was considered at  $p < 0.05$ . In addition, to test the probability of organ involvement in outcome, a survival analysis was performed providing Kaplan-Meier curves and significance of difference determined by a log-rank test, using the 1st tertile of MRI parameters as cut-off values.

For further details regarding the materials used, please refer to the [CTAT table](#).

### Results

The CC cohort ( $n = 60$ ) comprised 25 females and 35 males, aged  $60 \pm 9$  years, with a range of aetiologies, the largest being Alcoholic Liver Disease (ALD, 21 patients, 35%), Non-Alcoholic Fatty Liver Disease (NAFLD, 16 patients, 27%), and Hepatitis C Virus (HCV, 12 patients, 20%), with the remaining 18% of patients having primary biliary cirrhosis, Hepatitis B Virus (HBV), primary sclerosing cholangitis, autoimmune hepatitis and haemochromatosis. Mean model for end-stage liver disease (MELD) score, FIB4 and aspartate aminotransferase-to-platelet ratio index (APRI) scores were  $7.7 \pm 2.1$ ,  $3.4 \pm 2.3$ , and  $1.2 \pm 1.2$ . Of this group, six patients were on beta-blockers. The healthy volunteer (HV) group ( $n = 40$ ) comprised 17 female and 23 male patients, aged  $59 \pm 10$  years. The DC ( $n = 7$ ) group comprised five female and two male patients of  $48 \pm 13$  years, five of whom had ALD, one NAFLD and one HCV, with decompensation type comprising four cases of ascites, two of varices and one encephalopathy. Mean MELD, FIB4 and APRI scores were  $9.9 \pm 3.3$ ,  $3.5 \pm 1.6$ , and  $1.4 \pm 1.1$ , respectively.

### Validation of MR measures

#### *T<sub>1</sub> relaxometry of the liver*

$T_1$  relaxation time correlated significantly with visual morphometry of percentage fibrosis in advanced F4 fibrosis ( $R = 0.62$ ,  $p < 0.001$ ) (Fig. S2). As a secondary outcome, we show a significant positive correlation of liver tissue  $T_1$  with ELF score,  $R = 0.65$  and  $p < 0.001$  (Fig. S3). In addition, a highly significant correlation of liver tissue  $T_1$  with the LSM from FibroScan<sup>®</sup> was demonstrated ( $R = 0.68$ ,  $p < 0.001$ ) (Fig. S3).

#### *ASL perfusion of the liver*

In all patients ICG measures were collected and correlated with liver perfusion as measured by ASL. A weak but significant positive correlation was demonstrated between liver perfusion measured using ASL and ICG-PDR ( $R = 0.46$ ,  $p = 0.0016$ ), and negative correlation with ICGR15 ( $R = 0.46$ ,  $p = 0.0011$ ) (Fig. S4).

#### *Repeatability of multiparametric MRI measures*

Intra-subject repeatability for all the multiparametric MRI measures is provided (Table S1). Measurement of MR parameters is highly repeatable with a CoV of  $< 10\%$  in assessment of volume,  $T_1$  relaxometry measures, and ASL perfusion.

### Changes in compensated and decompensated cirrhosis compared to healthy volunteers

In the following section, MRI measures are provided for each organ studied – liver, spleen and SMA, renal and cardiac – and compared across the stages of disease severity, *i.e.* HV vs. CC vs. DC.

#### Liver

The changes measured in the liver across the three groups are shown (Fig. 1). Liver volume was significantly greater in patients with CC compared to both HVs and those with DC ( $p = 0.006$ ). We observed liver tissue  $T_1$  progressively increased with disease severity, from HV to CC and DC ( $p < 0.001$ ), with statistically significant differences between the HV and CC group ( $p < 0.001$ ), and the CC and DC group ( $p = 0.01$ ). Portal vein CSA significantly increased in CC patients compared to HVs ( $p < 0.001$ ). The CSA of the hepatic artery increased with

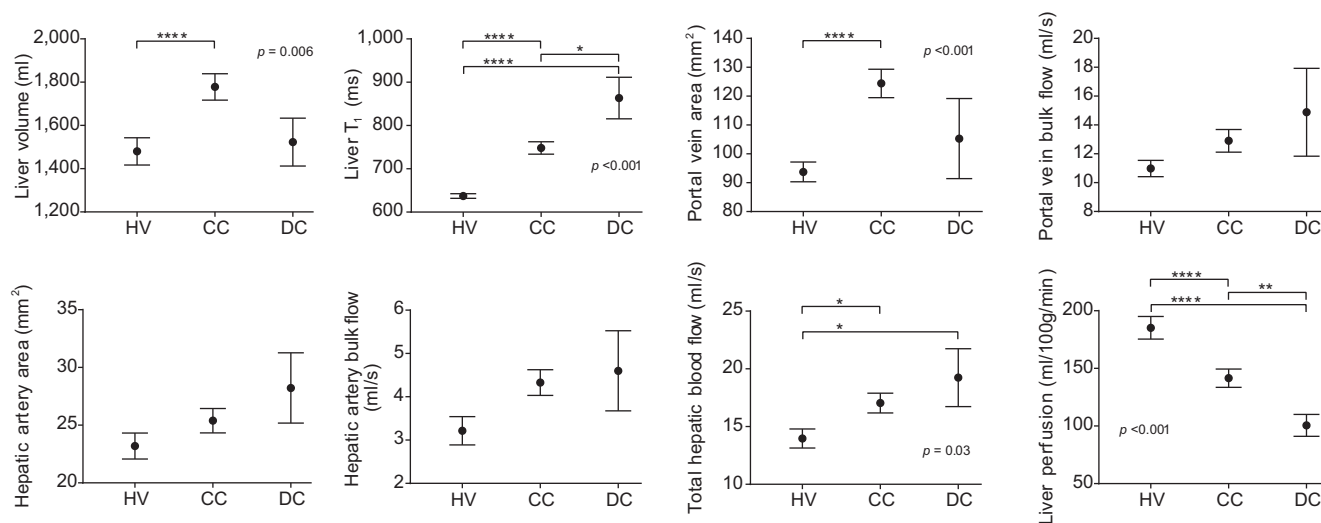


**Fig. 1. Changes in the liver in Healthy Volunteers, patients with Compensated Cirrhosis and those with Decompensated Cirrhosis.** Data analysed using one-way ANOVA, followed by the Tukey *post hoc* test. \* $p < 0.05$ , \*\* $p < 0.01$ , \*\*\* $p < 0.005$ , \*\*\*\* $p < 0.001$ . CC, Compensated Cirrhosis; CSA, cross-sectional area; DC, Decompensated Cirrhosis; HV, healthy volunteers.

disease severity (though not significant  $p = 0.09$ ). Total hepatic blood flow (portal vein + hepatic artery flow) significantly increased with disease severity ( $p = 0.03$ ). The percentage contribution of portal vein flow to total hepatic flow (portal vein flow + hepatic artery flow) did not significantly change with liver disease severity ( $77.9 \pm 1.2\%$ ,  $72.8 \pm 1.9\%$ , and  $74.5 \pm 6.7\%$  for HV, CC, and DC respectively). Liver perfusion significantly reduced with disease severity ( $p < 0.001$ ), with statistically significant differences between the HV and CC group ( $p < 0.001$ ), and the CC and DC groups ( $p < 0.01$ ).

### Spleen and SMA

Changes in the spleen and SMA across the groups are shown (Fig. 2). Spleen volume was increased in the CC and DC groups compared to HVs ( $p < 0.03$ ;  $206 \pm 16$  ml,  $459 \pm 34$  ml, and  $490 \pm 112$  ml for HV, CC, and DC respectively), with spleen  $T_1$  increasing with disease severity. No significant difference was found in CSA of the splenic artery, whilst splenic artery bulk flow significantly increased with disease severity ( $p < 0.001$ ). SMA bulk flow showed an increase with disease severity. Spleen

tissue perfusion significantly decreased with disease severity ( $p < 0.001$ ,  $151 \pm 7$  ml/100 g/min,  $120 \pm 6$  ml/100 g/min, and  $82 \pm 9$  ml/100 g/min for HV, CC, and DC respectively).

### Renal

Renal changes across the groups are shown (Fig. 3). No significant difference is seen in total renal volume between the HV, CC and DC groups. A significant reduction in renal cortex  $T_1$  ( $p < 0.001$ ) was demonstrated with disease severity, a trend for reduced  $T_1$  was found in the renal medulla but this was not significant. No significant difference was found in CSA of the renal artery or renal artery bulk flow, but flow per beat reduced with disease severity. No significant difference in renal cortex perfusion was found between the HV, CC, and DC groups.

### Cardiac

Differences in cardiac parameters across the groups are shown (Fig. 4). Cardiac index significantly increased with disease severity ( $p = 0.005$ ). This was driven by the increase in heart rate with disease severity ( $p < 0.001$ ,  $59.6 \pm 1.6$ ,  $67.2 \pm 1.6$ ,  $76.2 \pm 3.1$  beats

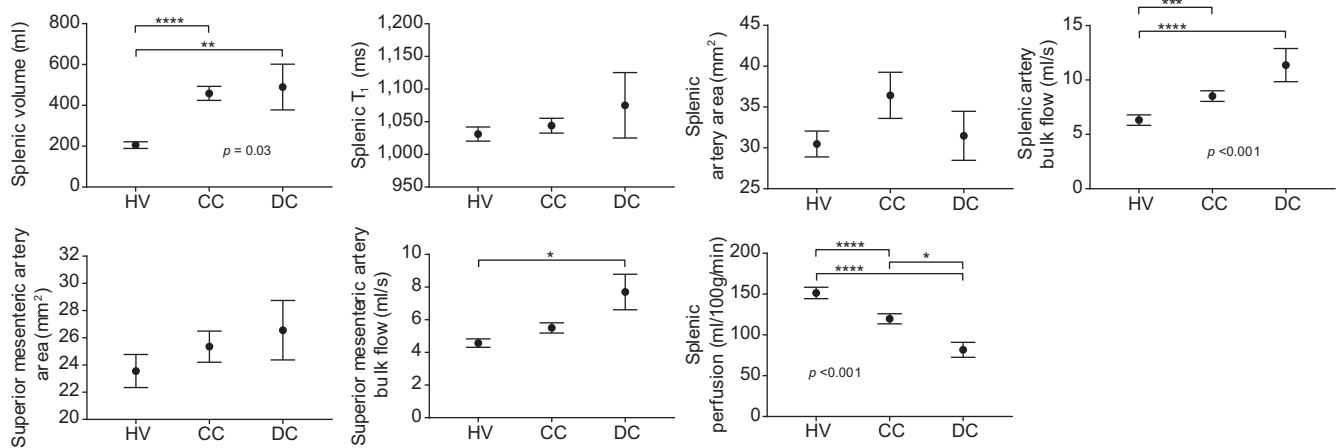


**Fig. 2. Changes in the spleen and superior mesenteric artery in Healthy Volunteers, patients with Compensated Cirrhosis and those with Decompensated Cirrhosis.** Data analysed using one-way ANOVA, followed by the Tukey *post hoc* test. \* $p < 0.05$ , \*\* $p < 0.01$ , \*\*\* $p < 0.005$ , \*\*\*\* $p < 0.001$ . CC, Compensated Cirrhosis; CSA, cross-sectional area; DC, Decompensated Cirrhosis; HV, Healthy Volunteers.

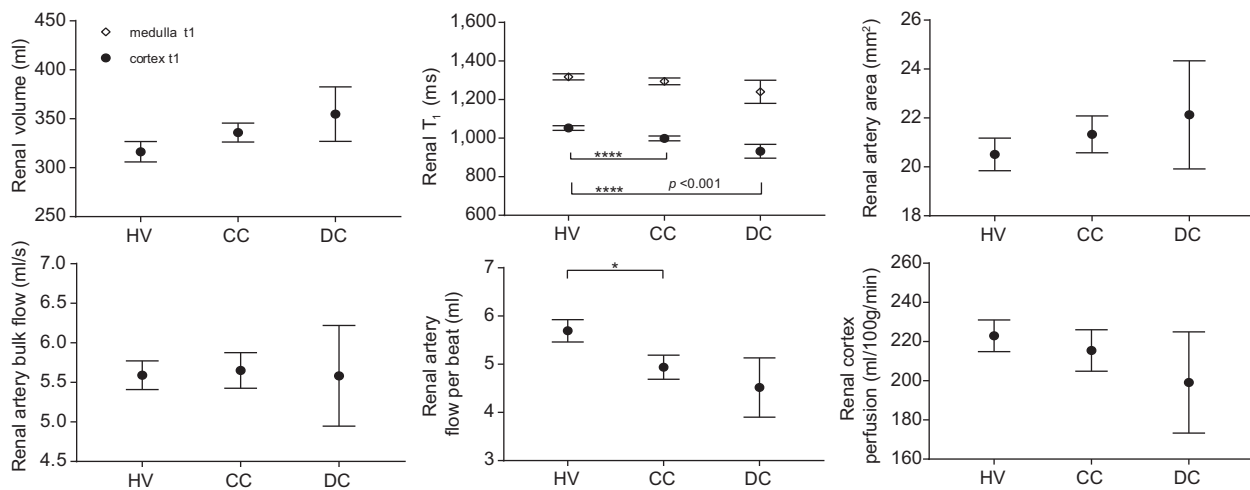


**Fig. 3. Changes in the kidney in healthy volunteers, patients with Compensated Cirrhosis and those with Decompensated Cirrhosis.** Data analysed using one-way ANOVA, followed by the Tukey *post hoc* test. \* $p < 0.05$ , \*\* $p < 0.01$ , \*\*\* $p < 0.005$ , \*\*\*\* $p < 0.001$ . CC, Compensated Cirrhosis; CSA, cross-sectional area; DC, Decompensated Cirrhosis; HV, Healthy Volunteers.

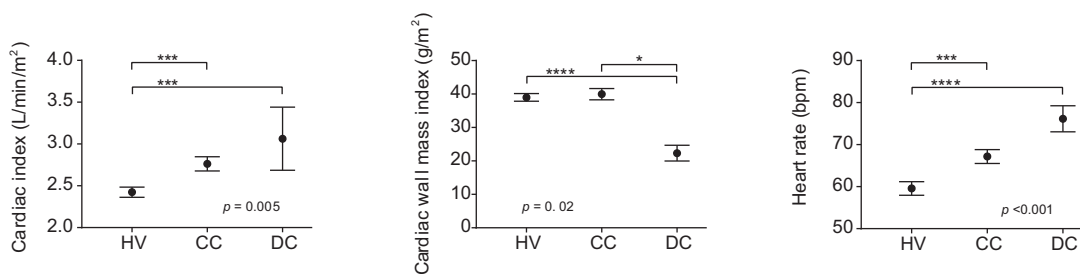


**Fig. 4. Changes in the cardiac function between healthy volunteers, patients with Compensated Cirrhosis and those with Decompensated Cirrhosis.** Data analysed using one-way ANOVA, followed by the Tukey *post hoc* test. \* $p < 0.05$ , \*\* $p < 0.01$ , \*\*\* $p < 0.005$ , \*\*\*\* $p < 0.001$ . CC, Compensated Cirrhosis; DC, Decompensated Cirrhosis; HV, Healthy Volunteers.

per minute (bpm) for HV, CC, and DC, respectively), no significant change in stroke volume was found with disease severity. BSA corrected cardiac LV wall mass was significantly different across the groups ( $p = 0.02$ ;  $39.0 \pm 1.1$ ,  $34.0 \pm 1.7$ ,  $22.3 \pm 2.4$  g/m<sup>2</sup> for HV, CC, and DC respectively).

**Assessment of baseline MR parameters related to a future clinical outcome in patients with compensated cirrhosis at baseline**

Here, we present baseline MRI data for those patients with CC who developed a liver-related outcome. Of the 60 patients with CC at baseline (mean MELD score 7.7), 11 patients (18%) developed a future liver-related outcome. The median number of days from MRI scan to a liver-related outcome was 1,001

(range: 59–2,304). Seven had ascites, one developed encephalopathy, one developed a variceal bleed, two had HCC. Of these patients, seven patients died of a liver-related cause after the first liver-related outcome; liver failure (four cases) and HCC (three cases) as listed on the death certificate.

The patients with an outcome were aged  $59 \pm 6$  years, six were male and five female, with aetiologies including four with HCV, five with ALD, one with NAFLD and one with HBV. How the MR parameters found to be significantly different between HVs, CC and DC patients relate to clinical liver-related outcomes is displayed (Fig. 5).

There was no significant difference in liver volume between patients with CC with and without a liver-related outcome. In contrast, liver tissue T<sub>1</sub> was significantly higher ( $p = 0.01$ ) in

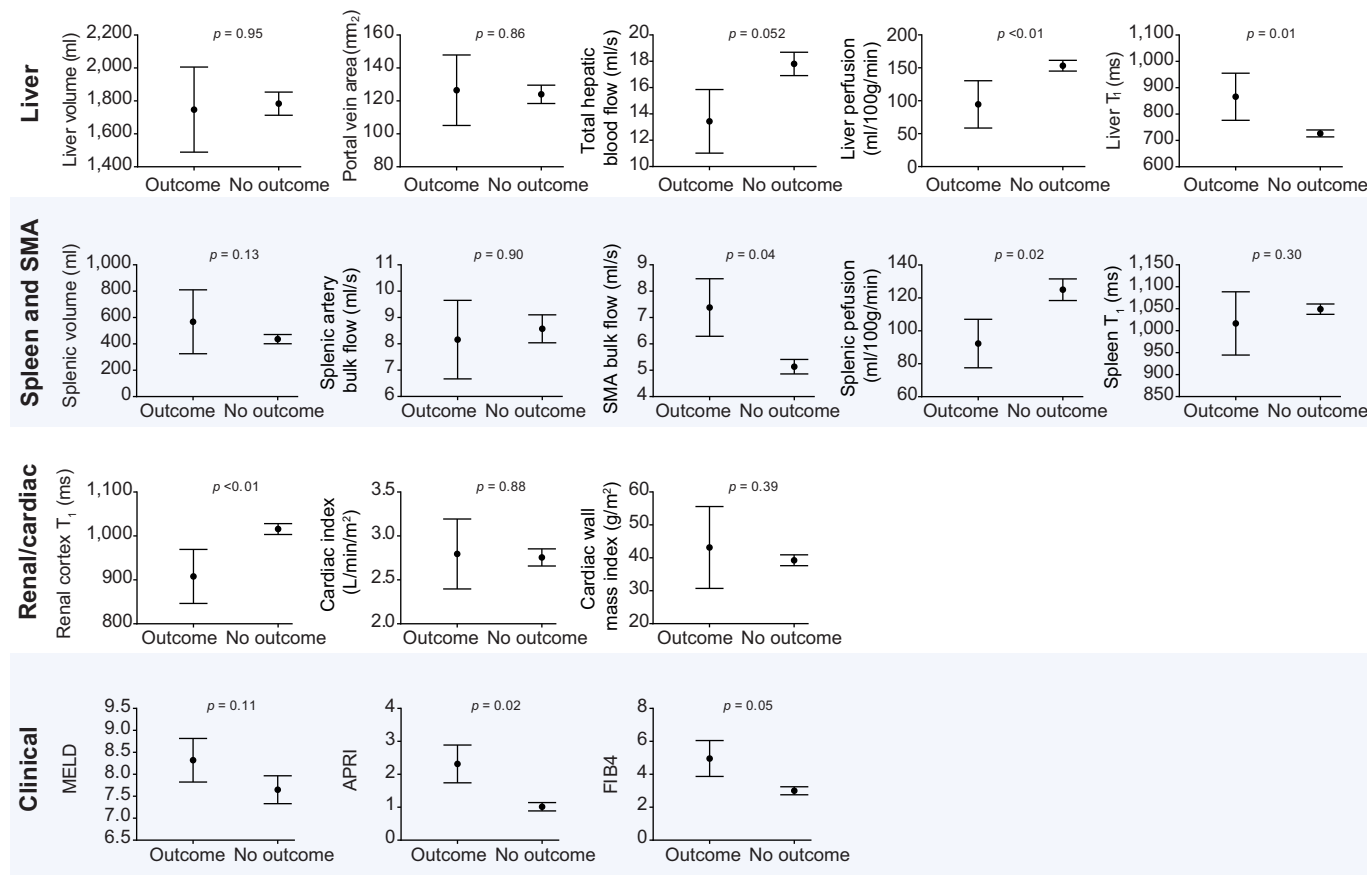


**Fig. 5. Baseline MRI parameters in patients with Compensated Cirrhosis, with and without liver-related outcomes.** APRI, aspartate aminotransferase-to-platelet ratio index; CC, Compensated Cirrhosis; FIB4, fibrosis 4 score; MELD, model for end-stage liver disease; SMA, superior mesenteric arterial. Statistical analysis performed using two-tailed unpaired t-test.

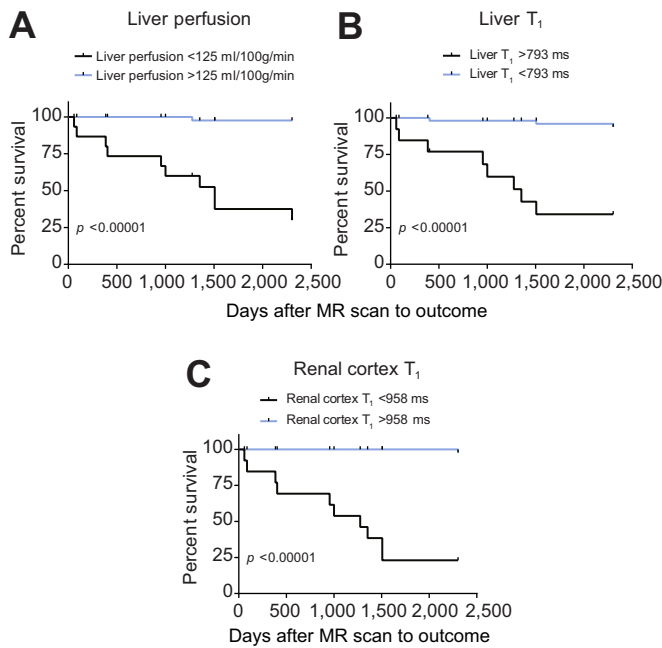


**Fig. 6. Kaplan-Meier curves for liver-related outcome survival in patients with Compensated Cirrhosis.** (A) There were significant differences between those with Liver T<sub>1</sub> for the 1st tertile T<sub>1</sub> of 793 ms ( $p < 0.001$ ). (B) There was significance between liver perfusion using the 1st tertile of 125 ml/100 g/min ( $p < 0.001$ ). (C) There was a significant difference between renal T<sub>1</sub> using a 1st tertile of 958 ms ( $p < 0.001$ ).

those patients with CC and a clinical outcome ( $834 \pm 36$  ms) compared to those without ( $719 \pm 10$  ms). The CSA of the portal vein was not significantly different between patients with CC, with and without a clinical outcome. Total hepatic blood flow was significantly ( $p = 0.05$ ) lower in those with outcomes ( $13.4 \pm 7.6$  ml/s) compared to those patients with no outcomes ( $17.8 \pm 6.0$  ml/s). Perfusion measured in the right lobe of the liver was significantly lower ( $p < 0.01$ ) in those patients with an outcome (clinical liver-related outcome:  $95.8 \pm 9.5$  ml/100 g/min, no liver-related outcome:  $160 \pm 8.0$  ml/100 g/min).

No significant difference was found in spleen volume or splenic T<sub>1</sub> between those with and without outcomes, but splenic perfusion was lower and SMA blood flow higher in those with a clinical outcome. Renal cortex T<sub>1</sub> was significantly shorter in the patients with CC and an outcome ( $919 \pm 28$  ms) compared to those with no outcome ( $1,012 \pm 11$  ms). There was no significant difference in cardiac measures of cardiac index or LV wall mass index between those with and without a clinical outcome. Tertile cut-off points (as used in<sup>23</sup>) of liver perfusion, liver T<sub>1</sub> and renal T<sub>1</sub> were used to compute Kaplan-Meier survival curves (Fig. 6). These MRI parameters were significant predictors of liver-related outcomes.

**Discussion**

We have shown that it is feasible to study changes in cirrhosis representing the flow, volume, composition and perfusion in critical organs (liver, kidney, spleen and heart) in a contemporaneous fashion in a single scan session using quantitative MRI without requiring the injection of a contrast agent. Individual MR components change with disease severity, as illustrated by Fig. 7, and taken together this data provides a comprehensive evaluation of cirrhosis relating to aspects of structure and haemodynamics. Furthermore, a subset of MRI markers measured at baseline (i.e. liver T<sub>1</sub>, liver perfusion and renal cortex T<sub>1</sub>) differentiate two groups of patients with CC, those who develop or do not develop a future liver-related clinical outcome up to seven years later (Figs. 5, 6).

This study highlights two conceptual aspects that are coherent with our current understanding of how liver disease progresses. Firstly, structural changes as evidenced by changes in organ volume (i.e. spleen and liver) and compositional change (i.e. increased liver T<sub>1</sub> and splenic T<sub>1</sub>) relate to increasing disease progression from the spectrum of HVs to DC. Secondly, changes in haemodynamics, both to and within the organ, evolve with progressive disease. This is exemplified by the reduction in both liver and splenic perfusion. Despite the small size of the DC group, it is interesting to note that the reduction of hepatic perfusion occurs in the context of increased total hepatic blood delivery in the CC and DC group, though this only results in



**Fig. 7. Multi-organ changes demonstrated in this study in compensated and decompensated liver disease.** Infographic to pictorially illustrate the changes in key organs (heart, liver, splanchnic and kidney) demonstrated in this study of contemporaneous MR measures in compensated and decompensated cirrhosis. A hyperdynamic circulation results in increased blood flow in the liver, splanchnic circulation and increased cardiac output in patients with CC, with further increases in spleen blood flow and cardiac index in patients with DC. Here liver and splenic perfusion was shown to be reduced in patients with CC compared to the HV group, and perfusion in these organs is further reduced in those with DC. No significant change in renal perfusion was found between patients with CC and DC, and the HV group. Liver tissue T<sub>1</sub> increased in patients with CC compared to HVs, and further increased in those with DC. Spleen T<sub>1</sub> was only significantly different from the HV group in DC patients. In contrast renal T<sub>1</sub> was reduced in patients with CC and further reduced in those with DC, compared to HVs. LV wall mass was significantly reduced in patients with DC compared to HVs, whilst liver volume was found to increase only in patients with CC, and spleen volume was increased in patients with CC and DC compared to HVs. CC, Compensated Cirrhosis; DC, Decompensated Cirrhosis; HV, Healthy Volunteers.

an increase in normalised hepatic blood flow between the HV and DC group (Fig. S5). The reduction in liver volume that occurs in DC compared to CC patients, as previously shown in,<sup>24</sup> suggests that this is not related to a larger mass of liver tissue to supply. We hypothesise two explanations for this discordance. Firstly, intrahepatic shunting may occur, although using our current MR methods we do not have the spatial resolution to directly visualise shunts. Secondly, in liver disease it is difficult to use normalised hepatic blood flow as a measure of global perfusion due to the underlying changes in liver composition. The deposition of fat, interstitial oedema and inflammatory cells can all potentially increase liver volume. As the liver starts decompensating, these features subside and in addition there is a loss of hepatocyte volume relative to an increasing amount of extracellular matrix.<sup>25</sup> This highlights the importance of measuring perfusion rather than blood flow *per se*.

The increase in splenic artery blood flow is largely compensated for by the increase in spleen volume, with a trend for a reduction in normalised splenic flow (Fig. S5) in agreement with the significant reduction in perfusion. The increase in splenic  $T_1$  also suggests that angio-architectural changes occur within the spleen, perhaps related to fibrosis. Finally, there was a trend for reduced renal perfusion, in the context of maintained renal artery bulk flow and increased kidney volume, in agreement with a reduced normalised renal blood flow (Fig. S5).

Of the 60 patients with CC, six were on beta-blockers, with this sub-group showing a significant reduction in splenic artery CSA, mean velocity and flux, spleen perfusion and portal vein mean velocity, thus increasing the CC cohort group variance in these measures. In addition, the DC sample size is currently underpowered to determine significant incremental changes, except in  $T_1$  relaxometry measures; this remains a work in progress.

The significant difference in baseline MRI parameters in those patients at risk of clinical events, within an average follow-up period of three years and maximum follow-up of seven years, is very encouraging. In this study 18% (11) of patients had a negative clinical outcome, this is a similar sample size to a recent study of events using multiparametric MRI of the liver alone and an associated liver inflammation and fibrosis score in which 10 patients (11%) were studied.<sup>26</sup> In the current study, we had more liver-related outcomes compared with previous studies (4% in a transient elastography study<sup>27</sup> and 13% in an ELF study<sup>28</sup>). The increased liver  $T_1$  (a marker of structural severity) and reduced liver perfusion (a marker of haemodynamic severity) in patients with early compensated liver cirrhosis experiencing future liver-related clinical outcomes has biological plausibility and provides a link between surrogate bio-imaging signals and robust clinical end points. The relevance of the strong relationship of renal cortex  $T_1$  to both disease severity and clinical outcomes is novel. Two studies, in patients with cirrhosis, have suggested changes in  $T_1$  occur within the cortex of the kidney, but until now these studies have been based on signal intensity changes of  $T_1$ -weighted images,<sup>29,30</sup> with no quantitative measures of  $T_1$  relaxation times having previously been reported. These previous studies suggest that the mechanism and physiology of reduced renal cortex  $T_1$  is decreased water content in the renal cortex due to renal hypoperfusion. Whilst the overall blood flow to the kidneys was maintained in our study, there was both a trend toward reduced renal perfusion, reduced renal artery flow per beat decreased and kidney volume increased (Fig. 3), with a sig-

nificant reduction in normalised bulk renal blood between HVs and patients with CC (Fig. S5). Thus, it is intriguing to speculate that regional vasoconstriction, driven by neurohormonal mechanisms, accounted for differential water content and reduced  $T_1$ . If this is proven to be the case, this has direct implications for the treatment of hepatorenal syndrome.

The overall picture that emerges from this study is consistent with our current understanding of the hyperdynamic circulation and the peripheral arterial vasodilatation hypothesis.<sup>4</sup> With advancing liver disease, reflected by structural changes within the liver (prolonged liver  $T_1$  values, Fig. 1) and haemodynamic changes in the liver (reduced liver perfusion, Fig. 1), there is a predicted rise in portal pressure (calculated from MRI data as a surrogate measure of HVPG<sup>20</sup> shown in Fig. S6). Pooling of blood in the splanchnic circulation as evidenced by increased SMA bulk flow and splenic artery bulk flow (Fig. 2) perpetuates this raised portal pressure. To accommodate the reduced effective central volume, the cardiac index increases in association with a raised heart rate (Fig. 4). Importantly this compensatory mechanism may be fragile as highlighted by the reduced LV wall mass in DC in our study and by others.<sup>31</sup> The DC group, albeit small in number, were ambulatory in our study. It is plausible that acute insults, including sepsis, that lead to hospitalisation tip the balance of these compensatory mechanisms. Recently, it has been proposed that vasodilation occurs in a differential manner in regional beds. Using PC-MRI angiography, McAvoy and colleagues<sup>32</sup> found a reduction in total renal blood flow in patients with advanced liver disease compared to HVs but an increase in total hepatic blood flow and SMA flow. Our data supports this concept of differential visceral blood flow in cirrhosis.

Here we present validation of our MRI measures against the gold standard, showing the correlation of  $T_1$  with the continuous biopsy variable of visual morphometry in METAVIR fibrosis stage F4, in agreement with previous reports in the literature across a wider range of fibrosis scores obtained from histology.<sup>17,19</sup> Further, we show that liver perfusion assessed in this CC cohort shows a significant correlation with indocyanine green (ICG-PDR and ICGR15). A recent study<sup>33</sup> assessed ICG continuous clearance and HVPG measurement against 2D PC-MRI of portal venous and hepatic arterial flow. They were able to demonstrate useful correlates that suggest that further development of MRI protocols for liver blood flow would be beneficial. We acknowledge ICG-PDR and ICGR15 are surrogates and not true measures of perfusion. Formal ICG clearance would be the optimal method, but this requires invasive transjugular hepatic venous sampling and simultaneous peripheral arterial sampling in patients receiving a continuous peripheral ICG infusion, as such this invasive procedure is far less practical. Doppler ultrasound has been widely used to assess blood flow in liver disease,<sup>34,35</sup> and has the advantage of being widely available. However, disadvantages include intra- and inter-observer variation, with reported intra-class variation of 0.49<sup>36</sup> due to inadequate standardisation of protocols including anatomical site, doppler beam angle and operator experience. Annet *et al.* showed PC-MRI parameters have the sensitivity to detect a significant difference between HV and cirrhotics not reflected in doppler ultrasound.<sup>34</sup> Doppler ultrasound has been shown to underestimate blood flow and be less reproducible in comparison to PC-MRI,<sup>37</sup> here we have shown the CoV of PC-MRI to be less than 5% in HVs,<sup>38</sup> further MRI has been shown to be more reliable with respect to inter-observer variability than

duplex doppler ultrasound.<sup>39</sup> Several studies have used computed tomography to assess portal vein and hepatic artery blood flow, but this is limited by ionising radiation exposure.<sup>40</sup>

There are a number of clinical implications of this study. Firstly, understanding the benefit vs. risk of existing and emerging therapeutics. Beta-blockers are used as standard care in the setting of portal hypertension. However, non-selective beta-blockers may be potentially deleterious after a critical threshold or window period has been traversed. It remains unclear when exactly this occurs, but this is likely to be related to diminishing cardiac output and a reduction in renal blood flow.<sup>6</sup> The concept of using MR protocols to assess response to beta-blockers has been explored by the Edinburgh group. They used PC-MRI to show a significant reduction in cardiac output (as measured by superior aorta blood flow) but maintenance of blood flow in other vessels (SMA, portal vein, hepatic artery, azygous vein) four weeks after commencing beta-blocker therapy, though this was in a small cohort of patients who were heart rate responders ( $n = 9$ ).<sup>13</sup> Furthermore, using MRI protocols to assess novel drug compounds has been highlighted by the recent report of serelaxin providing therapeutic potential in renal dysfunction in cirrhosis. In this study selective renal vasodilation did not appear to be offset by a reduction in systemic blood pressure or hepatic perfusion.<sup>41</sup> Taken together with our findings, the vision should be to use MRI protocols to assess response at an individual level and thus provide tailored therapy which is effective and safe. A further potential application for this MRI protocol could be as a prognostic tool for overall liver outcomes or specific complications. There is a growing body of literature showing the promise of non-invasive markers of liver fibrosis for prognostic performance.<sup>42,43</sup> The ability of two simple scores FIB4 and APRI to differentiate outcomes in early CC, as reproduced in this study (Fig. 5) cautions against positioning MRI as a generic prognostic tool. However, the difference in parameters between patients with/without significant clinical outcomes suggests that there is potential to use these parameters for prediction, which would be an understandable ambition in the era of emerging anti-fibrotic compounds. Larger studies are required to determine clinical utility of these promising multiparametric measures related to liver-related outcomes.<sup>44</sup>

This study was designed as a proof of concept study to assess the feasibility of using MRI to assess different organs in cirrhosis and confirms this is possible. Importantly, the scan time for the present protocol is one hour. Whilst we have obviated the requirement for an intravenous contrast agent, the scan time can now be reduced by omitting parameters which have been found to be non-contributory. This will be important for patient compliance and reducing cost and burden on radiology service provision time for future implementation into clinical practice. Whilst the MR picture obtained provides an overview it is by no means an exclusive assessment of the hyperdynamic circulation. For example, the current protocol does not provide an assessment of systemic vascular resistance nor does it delineate intrahepatic shunts, which we have postulated to underpin the marked reduction in liver perfusion. We deliberately chose aspects of MRI measurements that have been validated previously by our group and others based on comparison to gold standard reference tests including invasive angiography and liver biopsy. The current imaging protocol has been performed on 1.5 T but can easily be applied at 3 T, which provides higher signal-to-noise ratio and spatial resolution. Demonstrating that monitoring of therapy with MRI protocols can change hard

clinical outcomes and is cost effective within a multicentred randomised controlled trial will be required before considering implementation into clinical care.

We have shown that quantitative MRI can provide a global picture of cirrhosis by measuring aspects of flow, volume, composition and perfusion in critical organs. The change of key parameters including liver  $T_1$ , liver perfusion and renal cortical  $T_1$  in both progressive disease and in liver-related clinical outcomes has tangible utility in the understanding and treatment of the complications of chronic liver disease.

### Financial support

Financial support was received from the NIHR Biomedical Research Centre (NIHR BRC); Gastrointestinal and Liver Disorder Theme, Nottingham University Hospitals NHS Trust and University of Nottingham. This article presents independent research funded and supported by the NIHR Nottingham Digestive Diseases Biomedical Research Unit, Nottingham University Hospitals NHS Trust and University of Nottingham. Views expressed are those of the authors and not necessarily those of the NHS, NIHR or Department of Health.

### Conflict of interest

The authors declare no conflicts of interest that pertain to this work.

Please refer to the accompanying ICMJE disclosure forms for further details.

### Authors' contributions

CRB (Acquisition, analysis and interpretation of data, statistical analysis, drafting of the manuscript), EFC (Acquisition, analysis and interpretation of data, critical revision of the manuscript), RS and PK (Acquisition of data and critical revision of the manuscript), MWJ and GPA (critical revision of the manuscript), STF (Study concept and design, acquisition, analysis, interpretation of data, statistical analysis, drafting of the manuscript), and ING (Study concept and design, interpretation of data, statistical analysis, drafting of the manuscript).

### Acknowledgments

We would like to thank the NIHR Nottingham BRC research nurses, including Antonella Ghezi, Andrea Bennett, Tracey Wildsmith and Louise James who conducted patient enrolment and performed clinical measures, and Rubie-Jo Barker who produced illustrations.

### Supplementary data

Supplementary data associated with this article can be found, in the online version, at <https://doi.org/10.1016/j.jhep.2018.05.037>.

### References

*Author names in bold designate shared co-first authorship*

- [1] **Iwakiri Y, Groszmann RJ.** The hyperdynamic circulation of chronic liver diseases: from the patient to the molecule. *Hepatology* 2006;43(2 Suppl 1):S121–S131.

- [2] Møller S, Henriksen JH. Cardiovascular complications of cirrhosis. *Gut* 2008;57(2):268–278.
- [3] Schrier RW, Arroyo V, Bernardi M, Epstein M, Henriksen JH, Rodés J. Peripheral arterial vasodilation hypothesis: a proposal for the initiation of renal sodium and water retention in cirrhosis. *Hepatology* 1988;8(5):1151–1157.
- [4] Moller S, Bendtsen F. The pathophysiology of arterial vasodilatation and hyperdynamic circulation in cirrhosis. *Liver Int* 2018;38(4):570–580.
- [5] Taylor CR, McCauley TR. Magnetic resonance imaging in the evaluation of the portal venous system. *J Clin Gastroenterol* 1992;14(3):268–273.
- [6] Krag A, Bendtsen F, Henriksen JH, Moller S. Low cardiac output predicts development of hepatorenal syndrome and survival in patients with cirrhosis and ascites. *Gut* 2010;59(1):105–110.
- [7] Lauth WW. Regulatory processes interacting to maintain hepatic blood flow constancy: vascular compliance, hepatic arterial buffer response, hepatorenal reflex, liver regeneration, escape from vasoconstriction. *Hepatol Res* 2007;37(11):891–903.
- [8] Blendis L, Kreef L, Williams R. The coeliac axis and its branches in splenomegaly and liver disease. *Gut* 1969;10(2):85–90.
- [9] Zeng D, Dai C, Lu S, He N, Wang W, Li H. Abnormal splenic artery diameter/hepatic artery diameter ratio in cirrhosis-induced portal hypertension. *World J Gastroenterol* 2013;19(8):1292–1298.
- [10] Colecchia A, Montrone L, Scialoi E, Bacchi-Reggiani ML, Colli A, Casazza G, et al. Measurement of spleen stiffness to evaluate portal hypertension and the presence of esophageal varices in patients with HCV-related cirrhosis. *Gastroenterology* 2012;143(3):646–654.
- [11] Takuma Y, Nouse K, Morimoto Y, Tomokuni J, Sahara A, Toshikuni N, et al. Measurement of spleen stiffness by acoustic radiation force impulse imaging identifies cirrhotic patients with esophageal varices. *Gastroenterology* 2013;144(1):92–101, e2.
- [12] Reiberger T, Mandorfer M. Beta adrenergic blockade and decompensated cirrhosis. *J Hepatol* 2017;66(4):849–859.
- [13] McDonald N, Lilburn DML, Lachlan NJ, Macnaught G, Patel D, Jayaswal ANA, et al. Assessment of haemodynamic response to nonselective beta-blockers in portal hypertension by phase-contrast magnetic resonance angiography. *Biomed Res Int* 2017;2017:9281450.
- [14] Applegate GR, Thaete FL, Meyers SP, Davis PL, Talagala SL, Recht M, et al. Blood flow in the portal vein: velocity quantitation with phase-contrast MR angiography. *Radiology* 1993;187(1):253–256.
- [15] Gardener AG, Francis ST. Multislice perfusion of the kidneys using parallel imaging: image acquisition and analysis strategies. *Magn Reson Med* 2010;63(6):1627–1636.
- [16] Cox EF, Buchanan CE, Bradley CR, Prestwich B, Mahmoud H, Taal M, et al. Multiparametric renal magnetic resonance imaging: validation, interventions, and alterations in chronic kidney disease. *Front Physiol* 2017;8:696.
- [17] Agrawal S, Hoad CL, Francis ST, Guha IN, Kaye P, Aithal GP. Visual morphometry and three non-invasive markers in the evaluation of liver fibrosis in chronic liver disease. *Scand J Gastroenterol* 2017;52(1):107–115.
- [18] Heye T, Yang S, Bock M, Brost S, Weigand K, Longerich T, et al. MR relaxometry of the liver: significant elevation of T1 relaxation time in patients with liver cirrhosis. *Eur Radiol* 2012;22(6):1224–1232.
- [19] Hoad CL, Palaniyappan N, Kaye P, Chernova Y, James MW, Costigan C, et al. A study of T(1) relaxation time as a measure of liver fibrosis and the influence of confounding histological factors. *NMR Biomed* 2015;28(6):706–714.
- [20] Palaniyappan N, Cox EF, Bradley CR, Scott R, Austin A, O'Neill R, et al. Non-invasive assessment of portal hypertension using quantitative magnetic resonance imaging. *J Hepatol* 2016;65(6):1131–1139.
- [21] Buxton RB, Frank LR, Wong EC, Siewert B, Warach S, Edelman RR. A general kinetic model for quantitative perfusion imaging with arterial spin labeling. *Magn Reson Med* 1998;40(3):383–396.
- [22] Natori S, Lai S, Finn JP, Gomes AS, Hundley WG, Jerosch-Herold M, et al. Cardiovascular function in multi-ethnic study of atherosclerosis: normal values by age, sex, and ethnicity. *AJR Am J Roentgenol* 2006;186(6 Suppl 2):S357–S365.
- [23] Banyersad SM, Fontana M, Maestrini V, Sado DM, Captur G, Petrie A, et al. T1 mapping and survival in systemic light-chain amyloidosis. *Eur Heart J* 2015;36(4):244–251.
- [24] Tong C, Xu X, Liu C, Zhang T, Qu K. Assessment of liver volume variation to evaluate liver function. *Front Med* 2012;6(4):421–427.
- [25] Williams MJ, Clouston AD, Forbes SJ. Links between hepatic fibrosis, ductular reaction, and progenitor cell expansion. *Gastroenterology* 2014;146(2):349–356.
- [26] Pavlides M, Banerjee R, Sellwood J, Kelly CJ, Robson MD, Booth JC, et al. Multiparametric magnetic resonance imaging predicts clinical outcomes in patients with chronic liver disease. *J Hepatol* 2016;64(2):308–315.
- [27] Pang JXQ, Zimmer S, Niu S, Crotty P, Tracey J, Pradhan F, et al. Liver stiffness by transient elastography predicts liver-related complications and mortality in patients with chronic liver disease. *PLoS One* 2014;9(4):e95776.
- [28] Parkes J, Roderick P, Harris S, Day C, Mutimer D, Collier J, et al. Enhanced liver fibrosis test can predict clinical outcomes in patients with chronic liver disease. *Gut* 2010;59(9):1245–1251.
- [29] Lee KS, Muñoz A, Báez AB, Ngo L, Rofsky NM, Pedrosa I. Corticomedullary differentiation on T1-Weighted MRI: comparison between cirrhotic and noncirrhotic patients. *J Magn Reson Imaging* 2012;35(3):644–649.
- [30] Yamada F, Amano Y, Hidaka F, Fukushima Y, Kumita S. Pseudonormal corticomedullary differentiation of the kidney assessed on T1-weighted imaging for chronic kidney disease patients with cirrhosis. *Magn Reson Med* 2015;14(3):165–171.
- [31] Merli M, Torromeo C, Giusto M, Iacovone G, Riggio O, Puddu E. Survival at 2 years among liver cirrhotic patients is influenced by left atrial volume and left ventricular mass. *Liver Int* 2017;37(5):700–706.
- [32] McAvoy NC. Editorial: increased cardiac output in cirrhosis - non-invasive assessment of regional blood flow by magnetic resonance angiography. *Aliment Pharmacol Ther* 2016;43(12):1342–1343.
- [33] Chouhan MD, Mookerjee RP, Bainbridge A, Punwani S, Jones H, Davies N, et al. Caval subtraction 2D phase-contrast MRI to measure total liver and hepatic arterial blood flow: proof-of-principle, correlation with portal hypertension severity and validation in patients with chronic liver disease. *Invest Radiol* 2017;52(3):170–176.
- [34] Annet L, Materne R, Danse E, Jamart J, Horsmans Y, Van Beers BE. Hepatic flow parameters measured with MR imaging and Doppler US: correlations with degree of cirrhosis and portal hypertension. *Radiology* 2003;229(2):409–414.
- [35] Popov D, Krasteva R, Ivanova R, Mateva L, Krastev Z. Doppler parameters of hepatic and renal hemodynamics in patients with liver cirrhosis. *Int J Nephrol* 2012;2012:961654.
- [36] Iwao T, Toyonaga A, Shigemori H, Oho K, Sumino M, Sato M, et al. Echo-Doppler measurements of portal vein and superior mesenteric artery blood flow in humans: inter- and intra-observer short-term reproducibility. *J Gastroenterol Hepatol* 1996;11(1):40–46.
- [37] Yzet T, Bouzerar R, Allart JD, Demuyneck F, Legallais C, Robert B, et al. Hepatic vascular flow measurements by phase contrast MRI and doppler echography: a comparative and reproducibility study. *J Magn Reson Imaging* 2010;31(3):579–588.
- [38] Chowdhury AH, Cox EF, Francis ST, Lobo DN. A randomized, controlled, double-blind crossover study on the effects of 2-L infusions of 0.9% saline and plasma-lyte(R) 148 on renal blood flow velocity and renal cortical tissue perfusion in healthy volunteers. *Ann Surg* 2012;256(1):18–24.
- [39] Vermeulen MAR, Ligthart-Melis GC, Buijsman R, Siroen MPC, van de Poll MCG, Boelens PG, et al. Accurate perioperative flow measurement of the portal vein and hepatic and renal artery: a role for preoperative MRI? *Eur J Radiol* 2012;81(9):2042–2048.
- [40] Motosugi U, Sou TH, Morisaka H, Sano K, Araki T. Multi-organ perfusion CT in the abdomen using a 320-detector row CT scanner: Preliminary results of perfusion changes in the liver, spleen, and pancreas of cirrhotic patients. *Eur J Radiol* 2012;81(10):2533–2537.
- [41] **Snowdon VK, Lachlan NJ, Hoy AM, Hadoke PWF, Semple SI, Patel D, et al.** Serelaxin as a potential treatment for renal dysfunction in cirrhosis: preclinical evaluation and results of a randomized phase 2 trial. *PLoS Med* 2017;14(2).
- [42] Angulo P, Bugianesi E, Bjornsson ES, Charatcharoenwitthaya P, Mills PR, Barrera F, et al. Simple noninvasive systems predict long-term outcomes of patients with nonalcoholic fatty liver disease. *Gastroenterology* 2013;145(4):782–799, e4.
- [43] Vergnol J, Foucher J, Terrebonne E, Bernard PH, Bail B, Merrouche W, et al. Noninvasive tests for fibrosis and liver stiffness predict 5-year outcomes of patients with chronic hepatitis C. *Gastroenterology* 2011;140(7):1970–1979, e1-3.
- [44] Chouhan MD, Ambler G, Mookerjee RP, Taylor SA. Multiparametric magnetic resonance imaging to predict clinical outcomes in patients with chronic liver disease: a cautionary note on a promising technique. *J Hepatol* 2017;66(2):455–457.